ChemPubSoc Europe

DOI: 10.1002/cphc.201402492

Strong Coupling and Laser Action of Ladder-Type Oligo(*p*-phenylene)s in a Microcavity

Michael Höfner,*[a] Björn Kobin,[b] Stefan Hecht,[b] and Fritz Henneberger[a]

We investigate the coupling of ladder-type quarterphenyl to the photon modes of a dielectric ZrO_x/SiO_x microcavity at ultraviolet wavelengths. For a relatively long cavity ($\approx$10 μm) with high-reflectivity mirrors (0.998), optically pumped laser action is demonstrated in the weak-coupling regime. We observe single-mode operation with a threshold of 0.4 mJ cm^{-2}. Strong coupling is achieved by using a short $\lambda/2$ cavity. We find pronounced anti-crossing features of the molecular (0,0) and (0,1) vibronic transitions and the cavity mode in angle-dependent reflectivity measurements providing Rabi splittings of (90$\pm$10) meV. All these features occur spectrally resonant to the exciton transition of ZnO demonstrating the potential of ladder-type oligo(*p*-phenylene)s for the construction of inorganic/organic hybrid microcavities.

1. Introduction

Exciton–photon interactions in microcavities are a subject of both fundamental and practical interest. In the weak-coupling regime, vertical-cavity surface-emitting lasing (VCSEL) can be attained with a variety of advantages compared to edge emitters, such as low-threshold and single-mode operation. Strong coupling is characterized by the formation of combined exciton–photon excitations called polaritons. Phenomena like parametric amplification, lasing without inversion or Bose–Einstein condensation have been demonstrated in this situation.[1–3] At the beginning, research in that area was dominated by inorganic semiconductors,[2,4–7] but organic materials have come into focus in recent years,[8–13] and even more fascinating properties are predicted for hybrid cavities combining inorganic and organic semiconductors.[14–17]

Here, we investigate ladder-type oligo(*p*-phenylene)s that offer various attractive features in the above context.[18–20] Because of their rigid planar geometry, these molecules exhibit mirror-type, weakly Stokes-shifted absorption and emission spectra featuring well-resolved vibronic progressions. The absorption coefficient is considerably larger than that of the respective oligo(*p*-phenylene)s with non-rigidified backbone and the fluorescence quantum yield reaches unity in solution. Moreover, the exciton transition of ladder-type quarterphenyl (L4P) and its spiro-derivatives is almost in resonance with that of ZnO, making these molecules excellent candidates for the design of hybrid microcavities.

[a] M. Höfner, Prof. Dr. F. Henneberger
Department of Physics, Humboldt-Universität zu Berlin
Newtonstr. 15, 12489 Berlin (Germany)
E-mail: michael.hoefner@physik.hu-berlin.de

[b] B. Kobin, Prof. Dr. S. Hecht
Department of Chemistry, Humboldt-Universität zu Berlin
Brook-Taylor-Str. 2, 12489 Berlin (Germany)

2. Results and Discussion

Figure 1 summarizes the relevant characteristics of the selected molecule and of the mirrors constituting the cavities. The absorption of L4P-Sp2 exhibits two dominant bands corresponding to the (0,0) and (0,1) vibronic contributions to the S_0–S_1 transition. Their separation of 190 meV is not much larger than the Rabi splitting expected in a cavity, that is, the photon mode can significantly mix with both states simultaneously.[21]

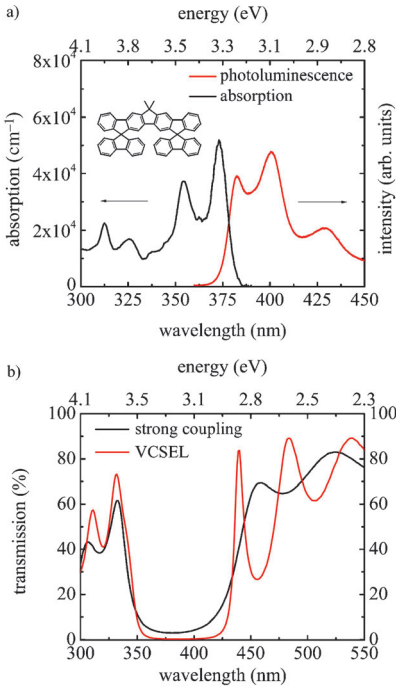

Figure 1. Components of the microcavities: a) Absorption and emission spectra of L4P-Sp2 in a polymer matrix. Inset: Structural formula of the molecule. b) Transmission spectra of the ZrO_x/SiO_x mirror stacks for strong coupling (black) and VCSEL (red).

The (0,0) feature in emission is reduced due to reabsorption and the stronger (1,0) transition thus favored for laser action. The thickness of the mirror layers is chosen such that the stop-band covers a range from (350–425) nm ensuring spectral overlap with the relevant emission and absorption features of L4P-Sp2 (Figure 1 b). The maximum reflectivity for the strong-coupling sample is 96.9% and 99.8% for the VCSEL structure. The stop-band is always centered at the (1,0) emission transition securing optimized conditions for laser action and providing a photon-mode that is low-energy-shifted with respect to both the (0,0) and (0,1) absorption resonances in the strong-coupling study.

2.1 Strong Coupling

The eigenstates of the cavity are indicated by minima in the reflection spectrum. Variation of the angle of incidence (θ) reveals the cavity dispersion curves, that is, the frequency ω as a function of the in-plane wavevector $k_{\parallel} = (\omega/c)\ \sin(\theta)$. Most simply, the normal component of the wavevector entering the roundtrip condition can be approximated by Equation (1):

$$k_z = [(\omega/c)^2 n^2_{\mathrm{eff}} - k_{\parallel}^2]^{1/2} \quad (1)$$

where n_{eff} is an effective refraction index of the whole cavity structure.[22] When discussed versus θ, the photon dispersion of the cavity without the molecular resonances is then given by Equation (2):

$$\omega_c(\theta) = \omega_c(0)/(1-\sin^2\theta/n^2_{\mathrm{eff}})^{1/2} \quad (2)$$

Figure 2 a depicts experimental reflectivity spectra of the sample designed for strong coupling. In addition to the photon mode, two further minima appear at larger incidence angles, with all three features showing clear anti-crossing behavior. The resultant three-branched dispersion curve is displayed in Figure 2 b. The data are well reproduced using a 3×3 Hamiltonian [Eq. (3)]:[17]

$$H = \begin{pmatrix} E_{00} & 0 & V_{01} \\ 0 & E_{01} & V_{00} \\ V_{01} & V_{00} & \hbar\omega_c(\theta) \end{pmatrix} \quad (3)$$

for three coupled oscillators. The energies $E_{00} = 3.32$ eV and $E_{01} = 3.51$ eV of L4P-Sp2 in absorption are independently determined from transmission measurements on a layer without mirrors (Figure 1 a), while the fit to the experimental data provides the coupling strengths $V_{00} \approx V_{01} \approx 45$ meV as well as $\hbar\omega_p(0) = 3.02$ eV and $n_{\mathrm{eff}} = 1.66$. The latter value is consistent with the refractive index of the polymer ($n = 1.6$), slightly enlarged because of contributions from L4P-Sp2 and the mirrors. The Rabi splitting given by the smallest separation of the minima in the spectra (Figure 2 a) occurring at the intersections of the uncoupled dispersions is 90 meV, both for the lower and middle as well as for the middle and upper branch, that is, twice the coupling strength.[10] As anticipated above, the polariton states of the middle branch are a mixture of all three oscillators with comparable weight in the vicinity of the intersections (Figure 2 d).

2.2 Laser Action

The system under study is a four-level laser, where the molecules are first pumped from the S_0 groundstate into higher vibronic excitations of S_1 and then rapidly relax to the lowest S_1 level. The subsequent (1,0) laser transition leaves the molecule in an excited vibrational state before it finally returns to the groundstate. This is concluded from the gain coefficient g determined independently on a single 120 nm-thick L4P-Sp2:polystyrene film spin-coated on a quartz substrate by the variable-stripe-length method. For two stripe lengths L_1 and L_2, Equation (4) holds:

$$[\exp(g L_1)\text{-}1]/[\exp(g L_2)\text{-}1] = I_1/I_2 \quad (4)$$

where I_1 and I_2 are the respective signals of the edge emission (Figure 3 a). Changing L_1 in the range of (200–250) μm while adjusting $L_1/L_2 \approx 2$ yields consistent data for g. Figure 3 a depicts the

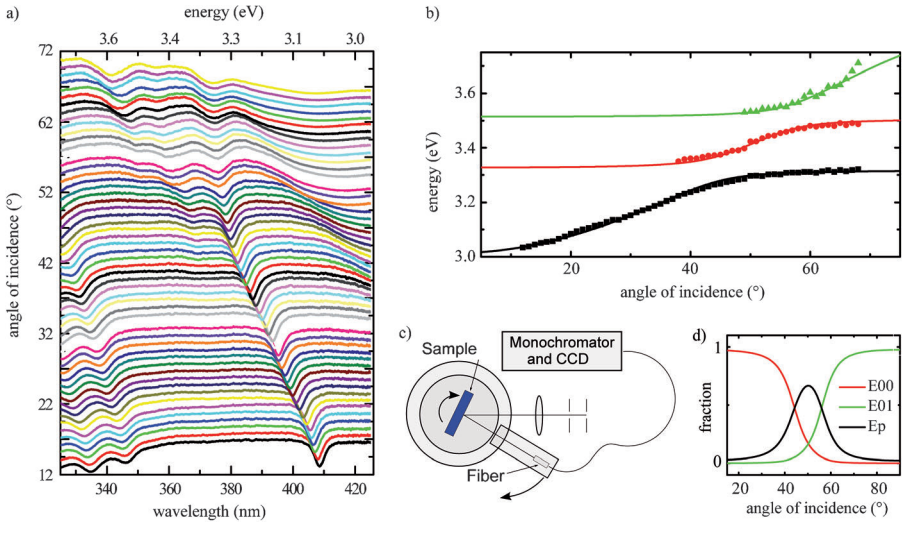

Figure 2. Strong coupling in a L4P-Sp2/ZrO_x/SiO_x microcavity: a) Cavity reflection spectrum at various angles of incidence θ varied in steps of 1° from 12° to 66°. The features at about 340 nm are Bragg modes of the cavity mirrors. b) Polariton dispersion curves deduced from (a). Dots: Experimental reflection minima. Curves: Three-coupled-oscillator model with a coupling strength of $V_{00} = 47$ meV and $V_{01} = 46$ meV, see text. c) Experimental geometry of the reflection measurement. d) Angle-dependent weights of the vibronic E_{00} and E_{01} states, as well as the cavity photon E_p calculated for the middle branch.

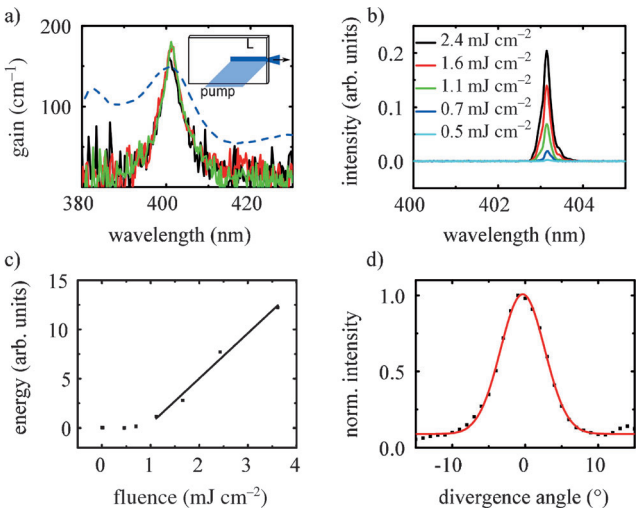

Figure 3. Laser action of L4p-Sp2/ZrO_x/SiO_x: a) Gain spectrum of an L4P-Sp2:polystyrene film pumped by an N2 laser at an energy density of 16 mJ cm^{-2} for various stripe lengths and spontaneous emission spectrum for reference (dashed blue). Inset: Pump scheme. b) Single-mode emission spectrum for different excitation densities as labeled. c) Spectrally integrated emission as a function of the pump fluence providing a threshold of (0.8 ± 0.1) mJ cm^{-2} (not corrected for pump light reflection). d) Angular emission divergence fitted to a Gaussian with a full width at half maximum of (7 ± 0.5)°.

gain spectrum at an excitation pulse fluence of Φ_p = 16 mJ cm^{-2}. The spectral profile is rather narrow and exhibits a prominent maximum of g_{max} = (170 ± 10) cm^{-1} at the (1,0) feature in spontaneous emission. In the air/film/quartz geometry, the modal gain g_{mod} is measured, which differs from the material gain $g_{mat} = g_{mod}/\Gamma$ by the confinement factor Γ. The relatively low g_{max} is thus a consequence of a poor gain-mode overlap in the reference film and larger gain coefficients are available in the cavity setting. The narrow spectral gain width is supportive of single-mode operation of the VCSEL structure, even though the spacing between two longitudinal modes is only about 3.5 nm at the 13 μm cavity length (deduced from Fabry-Perot oscillations next to the stop-band). Laser action at the (1,0) transition under optical pumping is evidenced by a steep increase of the emission signal (Figure 3b) with distinct threshold behavior (Figure 3c) as well as by a strong narrowing of the angular divergence of the emitted radiation (Figure 3d). Indeed, the spectral width of the laser emission of (0.3 ± 0.1) nm is markedly smaller than the mode spacing validating single-mode operation. Photodegradation is not an essential issue in the above measurements. Even after 10000 excitations, no change in the optical properties of the molecules is noticeable. A steady-state population of excited triplet states is reached, as proven by the occurrence of an emission spike when blocking and restarting the pulse train.

3. Conclusions

Ladder-type oligo(*p*-phenylene)s are well-suited organic molecules for optical applications at ultraviolet wavelengths. The Rabi splitting of about 90 meV observed in the strong-coupling regime can be further increased by using closely packed molecular films prepared, for example, by ultra-high-vacuum deposition. The VCSEL threshold of 0.4 mJ cm^{-2} (corrected for pump light reflection) is comparable to values reported in previous work on organic VCSEL structures in the visible spectral range.[23] The present cavities are not yet optimized and a reduction of the losses will likely enable a lowering of the lasing threshold. In particular, all the above features occur spectrally resonant to the exciton transition of ZnO where all-monolithic microcavities combining ZnO/ZnMgO Bragg mirrors and quantum well structures were demonstrated, capable of both strong coupling and VCSEL action.[5,24] From our results it is apparent that ladder-type oligo(*p*-phenylene)s and ZnO are an excellent combination for the fabrication of inorganic/organic hybrid microcavities. In this context, the formation of well-balanced polariton states, as shown above, is an important prerequisite, as it allows for engineering of the relaxation pathway along the branches and, by this, combining the strong photon coupling of the organic Frenkel excitons with the efficient scattering processes of the inorganic Wannier–Mott excitons.

Experimental Section

Microcavities are formed by alternating lambda-quarter stacks of ZrO_x and SiO_x layers fabricated by electron-beam evaporation. First, the bottom mirror is deposited on a soda lime glass platelet. The sample is then removed from the evaporator for preparing the molecular layer atop. Because of its improved photostability, the spiro-derivative L4P-Sp2 (details of the synthesis will be described elsewhere.) is selected as the active molecule (Figure 1a). Different procedures are now applied for the VCSEL structure and the strong-coupling cavity. For the latter, L4P-Sp2 and a cyclo-olefin-polymer (ZNX 480, Zeonex) are dissolved in toluene and spin-coated on the bottom mirror. The polymer is chosen because of its high glass transition temperature of 140 °C, compatible with the electron-beam evaporation. The resultant L4P-Sp2/ZNX480 film has a thickness of about 120 nm and contains 20 wt% of L4P-Sp2. After a drying time of one day, the sample is again placed in the evaporator and the top mirror is deposited. Both lower and upper mirror consist of seven ZrO_x and six SiO_x layers. For VCSEL operation, higher mirror reflectivities and a thicker active layer are needed to overcome the losses. Thicker stacks on the organic film suffer from increased inhomogeneities and tendency to rupture. Therefore, two mirrors with 11 layers of ZrO_x and ten layers of SiO_x are fabricated separately, as described before. Then, a solution of polystyrene (90 g L^{-1}) and 20 wt% L4P-Sp2 is dropped on one of the mirrors. After the solvent has evaporated, the second mirror is placed on top. The whole specimen is clamped together and heated to 120 °C for melting the polystyrene under light pressure. In this way, an active region of (10–15) μm thickness with good homogeneity and low interface roughness is obtained.

For angle-dependent reflectivity measurements, the sample is placed on a goniometer table and illuminated by a Xe lamp through two pinholes and a lens. The reflected light is collected by an optical fiber, passed into a monochromator, and detected with a charged coupled device (CCD). The setup allows for measurements with angles of incidence between 10° and 80°, with an accuracy of 0.5°. The high-excitation emission is studied in the same setting replacing the Xe lamp by a collimated N_2 laser providing 0.5 ns pulses with a repetition rate of 5 Hz at a wavelength of

337 nm. The sample is tilted relative to the excitation beam so that no stray light is coupled into the fiber. The gain is determined by the variable-stripe length method[21] on a 120 nm L4P-Sp2:polystyrene film with the same composition as that selected for the cavity but spin-coated on a quartz substrate to create a leaky waveguide. The N_2 laser is focused on a slit through a combination of a spherical and cylindrical lens, which is imaged on the sample's surface using a 80 mm lens creating a homogeneous stripe of well-defined length. The emission is collected from the edge of the sample, focussed on a monochromator, and detected with a CCD camera. All measurements are performed at room temperature.

Acknowledgements

The authors thank Simon Halm for preliminary measurements and fruitful discussions, Elfriede Renger for her support in the sample fabrication, and Moritz Stange for optical characterization of the mirror layers. This work was supported by the Deutsche Forschungsgemeinschaft (DFG) through IRTG 1740 as well as SFB 951 (HIOS) and by the São Paulo Research Foundation (FAPESP) through TRP 2011/50151-0.

Keywords: coupling · lasing molecules · microcavity · phenylenes · strong coupling

[1] J. Kasprzak, M. Richard, S. Kundermann, A. Baas, P. Jeambrun, J. M. J. Keeling, F. M. Marchetti, M. H. Szymańska, R. André, J. L. Staehli, V. Savona, P. B. Littlewood, B. Deveaud, L. S. Dang, *Nature* **2006**, *443*, 409 – 414.
[2] M. S. Skolnick, T. A. Fisher, D. M. Whittaker, *Semicond. Sci. Technol.* **1998**, *13*, 645.
[3] A. Kavokin, *Appl. Phys. A* **2007**, *89*, 241 – 246.
[4] Y. Yamamoto, F. Tassone, H. Cao in *Semiconductor Cavity Quantum Electrodynamics* (Eds.: J. Kühn, Th. Müller, A. Steiner, J. Trümper, P. Wölfle), Springer, Berlin, **2000**.
[5] S. Halm, S. Kalusniak, S. Sadofev, H.-J. Wünsche, F. Henneberger, *Appl. Phys. Lett.* **2011**, *99*, 181121.
[6] J. Wainstain, C. Delalande, D. Gendt, M. Voos, J. Bloch, V. Thierry-Mieg, R. Planel, *Phys. Rev. B* **1998**, *58*, 7269 – 7278.
[7] C. Weisbuch, M. Nishioka, A. Ishikawa, Y. Arakawa, *Phys. Rev. Lett.* **1992**, *69*, 3314 – 3317.
[8] R. J. Holmes, S. R. Forrest, *Org. Electron.* **2007**, *8*, 77 – 93.
[9] P. Schouwink, H. V. Berlepsch, L. Dähne, R. F. Mahrt, *Chem. Phys. Lett.* **2001**, *344*, 352 – 356.
[10] J. R. Tischler, M. S. Bradley, Q. Zhang, T. Atay, A. Nurmikko, V. Bulović, *Org. Electron.* **2007**, *8*, 94 – 113.
[11] D. G. Lidzey, D. D. C. Bradley, M. S. Skolnick, T. Virgili, S. Walker, D. M. Whittaker, *Nature* **1998**, *395*, 53 – 55.
[12] V. M. Agranovich, G. C. La Rocca, *Solid State Commun.* **2005**, *135*, 544 – 553.
[13] J. D. Plumhof, T. Stöferle, L. Mai, U. Scherf, R. F. Mahrt, *Nat. Mater.* **2014**, *13*, 247 – 252.
[14] H. Abassi, S. Jaziri, R. Bennaceur, *Phys. E* **2000**, *7*, 686 – 692.
[15] V. Agranovich, R. Atanasov, F. Bassani, *Solid State Commun.* **1994**, *92*, 295 – 301.
[16] V. Agranovich, H. Benisty, C. Weisbuch, *Solid State Commun.* **1997**, *102*, 631 – 636.
[17] J. Wenus, R. Parashkov, S. Ceccarelli, A. Brehier, J.-S. Lauret, M. S. Skolnick, E. Deleporte, D. G. Lidzey, *Phys. Rev. B* **2006**, *74*, 235212.
[18] M. Slootsky, X. Liu, V. M. Menon, S. R. Forrest, *Phys. Rev. Lett.* **2014**, *112*, 076401.
[19] U. Scherf, K. Müllen, *Makromol. Chem. Rapid Commun.* **1991**, *12*, 489 – 497.
[20] B. Kobin, L. Grubert, S. Blumstengel, F. Henneberger, S. Hecht, *J. Mater. Chem.* **2012**, *22*, 4383 – 4390.
[21] D. M. Coles, N. Somaschi, P. Michetti, C. Clark, P. G. Lagoudakis, P. G. Savvidis, D. G. Lidzey, *Nat. Mater.* **2014**, *13*, 712 – 719.
[22] Y. Wei, J. S. Lauret, L. Galmiche, P. Audebert, E. Deleporte, *Opt. Express* **2012**, *20*, 10399 – 10405.
[23] V. Bulović, V. G. Kozlov, V. B. Khalfin, S. R. Forrest, *Science* **1998**, *279*, 553 – 555.
[24] S. Kalusniak, S. Sadofev, S. Halm, F. Henneberger, *Appl. Phys. Lett.* **2011**, *98*, 011101.
[25] K. L. Shaklee, R. F. Leheny, R. E. Nahory, *Phys. Rev. Lett.* **1971**, *26*, 888 – 891.

Received: July 9, 2014
Published online on September 18, 2014